

Innovations in BER testers enable fast and accurate eye diagram, eye mask, Q-factor, and jitter measurements

Thomas A. Lindsay

*SyntheSys Research, Inc. 3475-D Edison Way, Menlo Park, CA 94025 U.S.A.
tlindsay@ieee.org*

Abstract: Successful integration of fast and accurate eye diagram, eye mask, jitter, and Q-factor functions into a BERT has been demonstrated. These measurements can be done with far greater speed and statistical accuracy than previously possible.

©2003 Optical Society of America

OCIS codes: (120.4800) Optical standards and testing; (060.2330) Fiber optics communications

1. Background

The most common tests performed on high-speed digital communications components and systems include eye diagram, eye mask, Q-factor, jitter, and bit error rate (BER) measurements.

Eye diagram, eye mask, and Q-factor tests are commonly done using a digital equivalent-time sampling oscilloscopes (ET scopes). Jitter measurements in the datacom industry are frequently made using ET scopes or time interval analysis techniques.

With architectural changes and careful design, it is possible to combine all these measurement functions into a BER tester. This paper reports on these new BERT methods, their challenges, and progress on performance.

2. Motivation

There are several important benefits of combining the additional measurement functions into a BERT.

- a. BER is the fundamental measure of quality for a digital communications link. Directly correlating the effects of jitter and amplitude degradations to BER assures system relevance to their measurements.
- b. The high sampling speed of the BERT improves quality by observation of low probability events and enabling more accurate extrapolation with higher confidence.
- c. Collection rates for eye diagrams and masks will rise by orders of magnitude to reduce critical test time.
- d. Test times will scale (except for a small fraction for processing overhead) with data rates. This means that future and faster data rates will provide even more speed and/or accuracy gains than with today's data rates.
- e. BERTs can study precise bit error locations and uncover error correlations, interferences and pattern sensitivities, even at very low error rates.
- f. Efficiency with fewer pieces of test equipment will result in less setup time, complexity, bench space, equipment cost, training, and data mismatch and confusion from multiple instruments. Further, a Pattern Generator (PG) may be required for some tests – most BERT testers have a PG built-in.

3. Innovations and principles of operation

Figure 1 shows a simplified block diagram for a BER receiver. Classically, the primary role of a BERT has been to confirm the operation of an upstream binary decision circuit. The threshold and delay settings could be coarsely centered in the input eye, and good performances of the comparator and flip-flop blocks were not imperative. Using new technology, BERT receivers can be enhanced to use the variable threshold and delay features to accurately and quickly scan bit error rate vertically (Q-factor), horizontally (jitter), and around mask perimeters (eye mask).

For the new test functions to be accurate, however, performances of the sampler, variable threshold and delay functions become critical. Many bit error decisions must be made with very small and transient amplitude differences (vs. the threshold) and at the precise moment of sampling. Considerations include:

- Comparator/sampler
 - High input return loss
 - Very fast, low noise, low hysteresis, low jitter, high gain
- Programmable threshold: high resolution, monotonic, linear, accurate; change quickly
- Programmable delay
 - Low jitter
 - High resolution, monotonic, linear, accurate; change quickly
 - Low wander for longer measurements
- Integrated processing, math & display to minimize overhead and take advantage of inherent speed

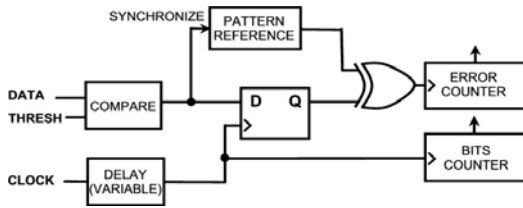


Fig. 1. Simplified block diagram for a BER receiver.

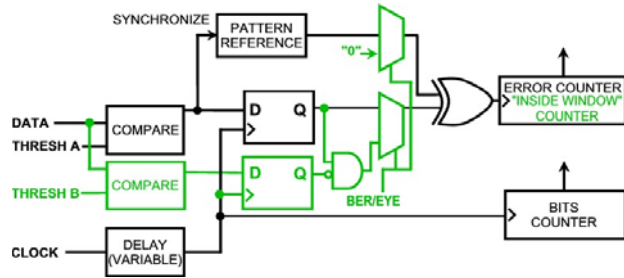


Fig. 2. BER receiver for eye diagramming

Figure 2 shows an architectural enhancement, whereby the instrument display is scanned with a window comparator function (and dedicated counter hardware) to create a two-dimensional histogram representation of the eye diagram. Then, with appropriate analysis algorithms, eye diagram measurements such as rise/fall times, amplitudes, over/undershoot, etc. are possible. In addition to those already listed above, the window comparator function brings more challenges: careful *matching* of return loss, delay, offset, response time, etc.

4. Experimental results

Experiments were set up to compare performances of an ET scope and a new BERT. The input waveform, from a PG output, was degraded by additive Gaussian noise and 20 feet of coaxial cable to introduce ISI. A PRBS7 pattern was used at a data rate of 1062.5 MBd.

4.1 Eye Mask

To compare the speed of eye mask testing, the masks were purposely shifted $\frac{1}{2}$ unit interval (UI) to the crossing so that violations would be detected quickly. Both the ET scope and the BERT counted mask hits for 10 seconds.

The ET scope and BERT eye mask results are shown in Figures 3 and 4, respectively. The ET scope accumulated 21,310 mask violations. The BERT, at 1062.5 MBd, counted 16,709,510 hits. Even when considering overhead for control and processing, the BERT showed nearly an 800x improvement over the scope. A BERT would accumulate even faster with higher data rates, whereas the scope's speed would be fixed.

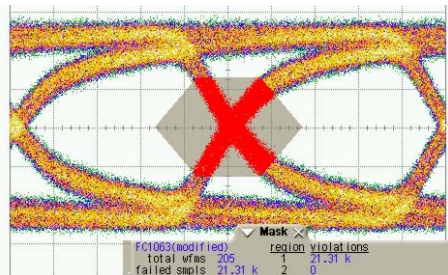


Fig 3. Mask violations for sampling scope.

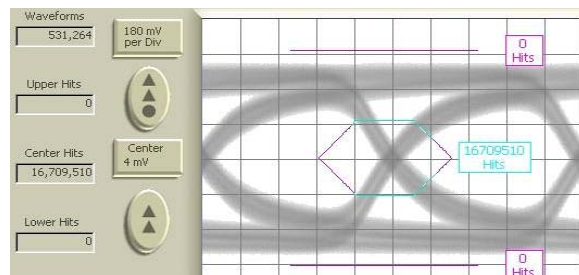


Fig. 4. Mask violations for BERT.

Additionally, the BERT showed almost 2600x gain in the mask waveform accumulation rate (531,264 vs. 205). Again, this improvement scales with data rate. To compare waveshapes, eye diagram rise times were measured on each instrument, with care to use the same definitions. The ET scope result was 369.5 psec, and the BERT's result was 366 psec, showing excellent agreement.

4.2 Jitter

ANSI standards [1] separate deterministic (DJ) and random (RJ) jitter using analysis of a model known as dual Dirac. In this model, the jitter probability density function (pdf) is approximated as the sum of two Gaussian functions. The time between the means ($\mu_l - \mu_r$) is defined as DJ, and RJ is defined as the average of the standard deviations (σ_l, σ_r). See Equation (1). Subscripts l and r represent left and right Gaussian functions, respectively.

$$J(t) := \frac{1}{2\sqrt{2\pi}} \left[\frac{e^{-\frac{(t-\mu_l)^2}{2\sigma_l^2}}}{\sigma_l} + \frac{e^{-\frac{(t-\mu_r)^2}{2\sigma_r^2}}}{\sigma_r} \right] \quad (1)$$

ANSI [1] defines total jitter (TJ) as the pk-pk value associated with a BER of 1E-12. For compliance, actual distributions must be fit to the model and the effective DJ and TJ values determined. Since deterministic jitter is usually a superposition of numerous individual distributions in the higher probability center area, it is important to collect measurements farther away from the center and towards the tail of the distribution where the pdf shape is more assured to be Gaussian and also where less extrapolation is required. Furthermore, because of effects of long patterns, rare events, or noise floors, the error of the curve-fit values versus the actual jitter value at 1E-12 BER depends largely on how close to that level data is actually collected.

Figure 5 shows a jitter display from the BERT. This test ran for 18 seconds and collected data down to the 1E-8 BER level at the 1062.5 MBd rate. Only data below 1E-4 was taken to reduce possible impact from deterministic effects. Actual measurement points are shown by black dots. DJ, (RJ), and TJ values are displayed.

For comparison, Figure 6 shows an ET scope jitter histogram. 18,780 hits were collect in 18 seconds. At this rate, it would take >26 hours to accumulate 1E8 samples. Since this is impractical, typical scope methods measure for a much shorter time, subsequently requiring extra extrapolation and likely more error.

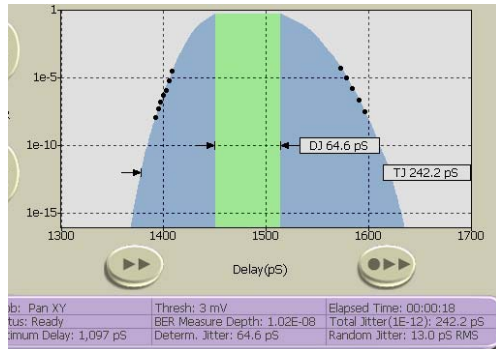


Fig. 5. Jitter measurement taken with a bit error rate tester.

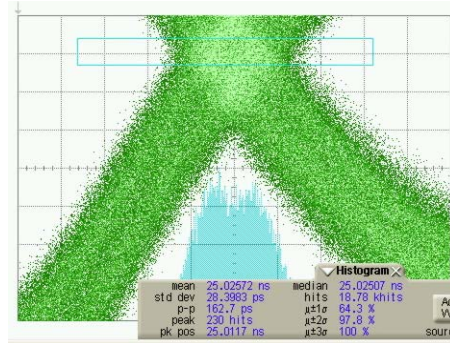


Fig. 6. Sampling scope jitter histogram.

The scope reports a rms jitter value of 28.4 psec and a pk-pk value of 162.7 psec. Compare this with the BERT's values of 13 psec for RJ and 242.2 psec for TJ at BER=1E-12 – the scope's rms reading does not correctly represent RJ due to the effects of ISI, and the short test time with low sample rate understates TJ. Note, the scope's pk-pk result does compare well with the 164.9 psec pk-pk difference of the BERT's upper readings, at BER~3E-5.

As stated above, the dual Dirac model is a probability density function. Per Annex A of the ANSI report [1], as a BERT scans each side of the pdf, it natively reports the cumulative distribution function (CDF), otherwise known as the time integral of the pdf. With t_d as the average transition density (0.5 for PRBS7),

$$\text{BER}_L(t) := t_d \cdot \int_{-\infty}^t J(t) dt \quad \text{and} \quad \text{BER}_R(t) := t_d \cdot \int_t^{\infty} J(t) dt \quad (2)$$

The BERT records several $\text{BER}_x(t)$ vs. sample-time (t) pairs for each side x of the pdf, shown as dots in Figure 5. The BER values are converted to equivalent Q values (# of Gaussian rms values from the mean) with a simple but accurate polynomial approximation for the inverse cumulative probability distribution. If the measured pdf is truly Gaussian over the measurement range, then the Q values and their associated times will form a straight line, which can be easily verified. A fitted line is then determined by a least-squares method. The reciprocal of the magnitude of the line's slope is σ_x for that side of the pdf, and the line's Y-intercept divided by the slope is $(-)\mu_x$ for that side of the pdf. From these, DJ and TJ (for 1E-12) are quickly calculated. Independent results of this process are shown in Figure 7, with virtually identical results to those displayed in Figure 5. The dual Dirac pdf and both CDFs are plotted. Note, this data is often displayed in a "jitter bathtub" format, wherein the 1/2 of the display is shifted 1 UI.

Math processing required for analyses is built into the tester in keeping with the objectives of higher speed, but data tables are also available for download and additional analysis, if desired.

For amplitude Q-factor (S/N) measurements, BER can be swept in much the same manner except by vertically varying the threshold instead of sweeping sampling time for jitter. Similar algorithms can be used to separate deterministic from Gaussian terms. Such separation is important, because if it is assumed that all the variation around a logic level is Gaussian, as is typically done in scopes, the rms value (N) will be overstated, and Q will be understated. For the tested waveform, the scope reported a Q factor of 5.73, whereas the BERT reported a Q-factor of 18.9. This difference is because the waveform had a fair amount of deterministic non-Gaussian closure due to ISI.

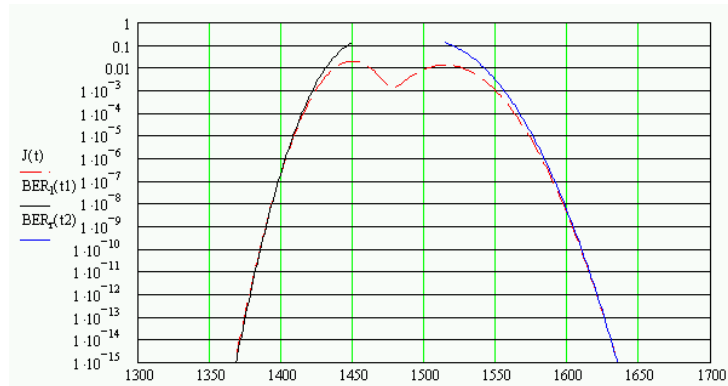


Fig. 7. Independent dual Dirac analysis of BERT jitter values.

5. Conclusions

The ability to overcome the stated challenges and successfully integrate accurate eye diagram, eye mask, jitter, and Q-factor functions with current BER and analysis capabilities has been demonstrated to greater than GBd data rates. These measurements can be done with greater speed and statistical measurement depth than previously possible, offering significant cost, time, and logistical advantages to design verification and manufacturing test systems.

Future development plans for BER technology include:

- Higher data rates to >12 GBd (and faster measurements).
- Performance improvements with new technologies for sampling, timing, and processing blocks.
- More advanced analyses such as BER-based eye contouring for improved accuracy.
- Additional features such as built in TDP and Stressed eye tests for 10G Ethernet and 10G Fibre Channel.

[1] *Information Technology - Fibre Channel - Methodologies for Jitter Specification*, Document Number: INCITS TR-25-1999, InterNational Committee for Information Technology Standards (formerly NCITS), 01-Sep-1999.